ORIGINAL PAPER

Numerical study on the influence of porous baffle interface and mesh typology on the silencer flow analysis

Giada Kyaw Oo D'Amore[1] · Mitja Morgut[1] · Marco Biot[1] · Francesco Mauro[2]

Abstract

The study of the internal component geometries (i.e. perforated elements) is relevant for the acoustic performance optimisation of a silencer. During the design phase, the evaluation of the properties of a silencer is performed by numerical analysis. In the literature, there is a lack of general guidelines and comparisons among different modelling strategies. So, in this study, the influence of grid type (i.e. trimmed vs tetrahedral) on the numerical prediction of the flow inside a reactive silencer is analysed. Moreover, using a porous baffle interface to model the perforated pipe is investigated, searching for a faster and easier way to model perforated elements. The simulations are carried out with the commercial CFD software STAR-CCM+. The comparison of the obtained axial velocity with a literature case study assesses the numerical model reliability. The analysis highlights that velocity and pressure predicted with both the mesh typologies does not significantly differ, but the trimmed mesh allows to save cells number, reducing the computational cost. Instead, obtain a reliable flow description using the porous baffle interface is strictly correlated to the settings of the resistance coefficient. This assumption does not provide accurate results for the analysed perforated pipe. On the other hand, using a simplified model allows to easily perform a comparison between different muffler geometries, as the holes have not to be drowned and meshed after each modification.

Keywords Muffler · CFD simulations · Porous baffle interface · Perforated pipes

1 Introduction

Silencers are a fundamental parts of engine exhaust systems and are commonly used to minimize the noise of the exhaust gases caused by the combustion inside the engine. The optimization of mufflers is necessary to meet the radiated noise levels (dB(a)) required by environmental regulations [1, 2]. Hence, this has become a relevant research area for several industrial sectors (e.g. automotive [3] and marine [4]) and the studies are usually performed by numerical simulations.

The muffler design affects noise characteristics, emissions and fuel efficiency of an engine; therefore, the good design of a muffler should guarantee the highest possible noise reduction while offering the minimum backpressure

✉ Giada Kyaw Oo D'Amore
  giada.kyawood'amore@phd.units.it

1 Department of Engineering and Architecture, University of Trieste, Via Alfonso Valerio 6, 34127 Trieste, Italy

2 Department of Naval Architecture, Maritime Safety Research Centre, Ocean and Marine Engineering, University of Strathclyde, Glasgow G4OLZ, Scotland, UK

[3]. Inside a muffle, cross-flow perforated pipes are the most significant acoustic noise reduction elements but are also the most critical components regarding backpressure [5]. In this sense, the holes diameter and the porosity of the perforated tube are the principal characterizing parameters [6].

Analyzing the available literature on CFD (computational fluid dynamics) simulations on mufflers [5, 7–13], it is not possible to derive a general guideline for the modelling approach as well as meshing strategy. Therefore, the primary aim of this preliminary study is focused on the investigation of the mesh typology (i.e. tetrahedral vs trimmed) influence on the simulated mean flow. Moreover, with the intention to develop a fast procedure for mufflers design, the use of the porous baffle interface to model the perforated elements is also investigated. In fact, the use of a porous baffle interface can save modelling and computational time during the muffler design process. In example, to investigate multiple holes' geometry or configurations, it is not necessary to re-draw and re-mesh the entire geometry, but is sufficient to modify the perforated pipe parameters inside the CFD solver; the porous baffle interface simulate the dissipation that occur when the flow pass through the holes starting

from the viscous and inertial resistance parameters used. These parameters have to be proper set in order to simulate a reliable cross-flow. On the other hand, with the adoption of a baffle interface, it is not possible to accurately reproduce the flow through the holes, being the porous pipe crossed by the fluid through the entire baffle length.

2 Materials and methods

The present study uses as reference geometry the muffler reported by [14] in Sect. 2.3 with an open area ratio (OAR) equal to 1.0; the OAR is expressed in Eq. (1):

$$OAR = \frac{4L\varepsilon}{d}, \tag{1}$$

where L and d are the length and the diameter of the perforated pipe respectively and ε is the overall porosity of the perforate expressed as follow [15]:

$$\varepsilon = \frac{A_{holes}}{A_{pipe}}, \tag{2}$$

where A_{holes} and A_{pipe} are the total hole area and the whole perforated pipe area respectively.

The muffler geometry used in this study is reported in Fig. 1. The inlet pipe, depicted in pink, goes on with a straight pipe, depicted in green, that ends with a plug, depicted in black. The blue part of the inner straight pipe represents the perforated section that connects the flow with the outer pipe, depicted in grey. The outer pipe ends with the outlet of the system, depicted in orange.

The perforated pipe has an overall porosity of 7%, a hole diameter of 3.00 mm and a thickness of 1.50 mm.

The software STAR-CCM+ is used to perform the CFD analysis. All the physical parameters and the boundary conditions are set following the case study chosen [14] in order to use the literature data as reference to evaluate the obtained results by the present study. The working medium utilized is air at 623 °C with a density of 0.39 kg m^{-3} and a viscosity of 4.0 e^{-5} kg (m s)$^{-1}$. A segregated and steady approach is used in the framework of the RANS (Reynolds Averaged Navier Stokes) simulations in combination with the k–ε turbulence

model as used in [14]. The boundary conditions are set up as reported in Table 1.

The domain is discretized with both tetrahedral and trimmed meshes (Fig. 2) using a base size chosen on the basis of the mesh sensitivity study presented in the next section. The prism layer is generated with a total thickness of 5.83 mm and 6 prism layers with a stretching factor of 1.5 in order to obtain a wall $y^+ \leq 1$. Working with a wall y^+ less than 1 no wall functions are used. A refining area is set around the perforated pipe, setting a target value of 20% of the base size for the generated cells; in Fig. 2 the section of the circular refining crown is highlighted in red. No other zones with different mesh size have been considered in order to avoid numerical diffusion: as a matter of fact, if cell size changes too quickly between adjacent cells, numerical errors will occur, so slow transitions between the refinement areas above described are needed. In order to decrease the computational effort, thanks to the muffler geometry, two symmetry planes have been used in the simulations; thus, only a quarter of the muffler has been modelled.

Considering the porous baffle interface used to model the perforated pipe, the viscous and inertial resistance parameters have to be set to proper model the cross-flow. The Darcy–Forchheimer law, reported in the following equation, is used to characterize the flow through a porous media [16]:

$$\frac{\Delta P}{L} = -\left(\nu\alpha + \frac{1}{2}V\beta\right)V, \tag{3}$$

where ΔP is the pressure drop, L is the length of the porous media, ν is the kinematic viscosity, V is the fluid velocity and α and β are the viscous and inertial resistance coefficient respectively. An expression for α and β, that depend on porous media properties such as porosity ε and particle size d_p, was proposed by Ergun [15]:
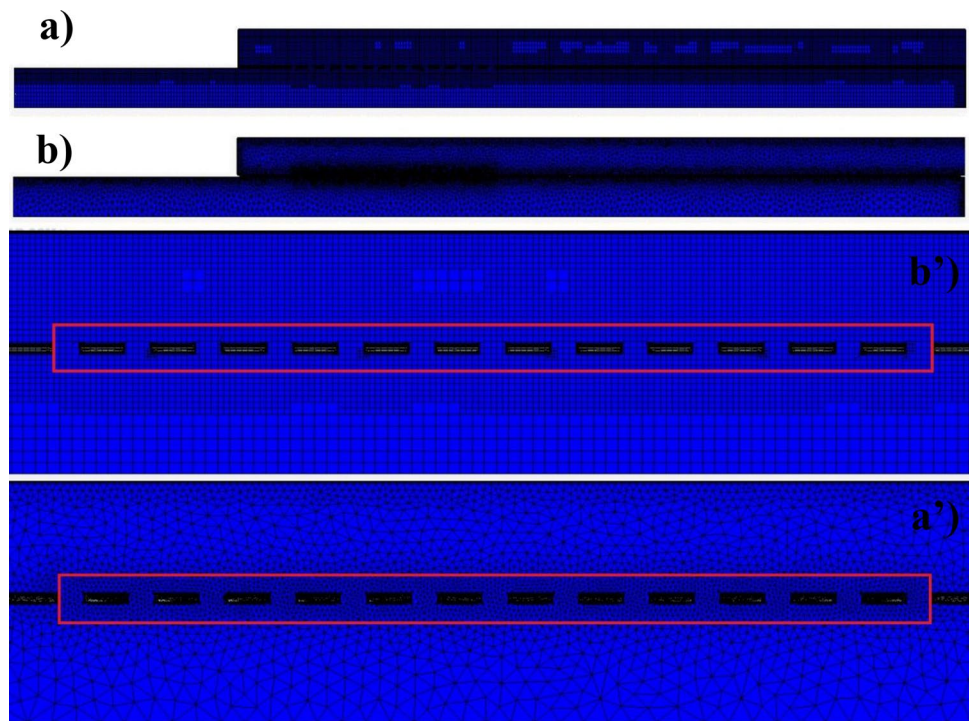
Table 1 Boundary conditions

	Boundary type	Value
Inlet	Velocity	60 m s^{-1}
Outlet	Pressure	101,325 Pa
Surfaces	Wall	No slip condition

Fig. 1 Muffler geometry, measures in mm
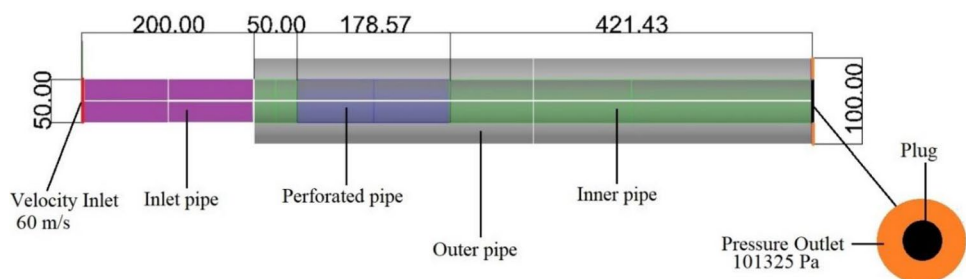
Fig. 2 **a** Trimmed mesh and **b** tetrahedral mesh on the symmetry plane; **a′**–**b′** zoom on the perforated pipe, refining area highlighted in red. Real geometry model

$$\alpha = \frac{150}{d_p^2} \frac{(1-\varepsilon)^2}{\varepsilon^3}, \tag{4}$$

$$\beta = \frac{1.75}{d_p} \frac{(1-\varepsilon)}{\varepsilon^3}. \tag{5}$$

These expressions are valid for cellular media, made of small sphered shapes particles. To this end, the perforated pipe can be compared to a cellular media, constituted by solid filaments connected to form pores. So, the equivalent particle diameter expressed in Eq. (5) is used to calculate α and β coefficients [17]:

$$d_e = 1.5 \frac{1-\varepsilon}{\varepsilon} d_c, \tag{6}$$

where d_c is the cylindrical form of the hydraulic diameter.

In this work, the only resistance parameter considered for the porous baffle interface is the inertial one, being the flow inside the muffler turbulent ($Re \sim 30{,}000$). The value of β coefficient calculated for this case study, using a d_e equal to 0.059 m, is 80,422 m^{-1}.

3 Mesh sensitivity study

The mesh sensitivity study is performed with the real geometry model and both the tetrahedral and the trimmed mesh. The pressure drop (ΔP) between the inlet and the outlet is

chosen as reference parameter and the base size is varied in the range 1.25–20.00 mm with a refinement ratio equal to 2. The asymptotic solution can be evaluated by the GCI (Grid Convergence Index) [18], expressed in the following equation:

$$\text{GCI} = 1.25 \left\{ \left(\frac{|F_{i+1} - F_i|}{F_i} \right) \left[\frac{1}{(r^p - 1)} \right] \right\}, \tag{7}$$

where r is the refinement ratio, F_i are the model values with i that decreases with the grid refinement and p the solution convergence order expressed in the following equation:

$$p = \ln\left(\frac{F_{i+2} - F_{i+1}}{F_{i+1} - F_i} \right) / \ln(r) \tag{8}$$

Comparing two successive values of GCI using the following equation, the asymptotic solution can be estimated: when the value of the parameter A_r is near to 1, the desired condition is satisfied.

$$A_r = r^p \left(\frac{\text{GCI}_i}{\text{GCI}_{i+1}} \right). \tag{9}$$

A perusal of Fig. 3 shows that decreasing the cell dimensions, the calculated ΔP reaches the convergence. A value of A_r equal to 1.0 is obtained considering $\text{GCI}_{2.5}$ and GCI_5 (Table 2) for both the tetrahedral mesh and the trimmed one. Accordingly, a mesh size of 5.0 mm is selected for the computations as it is in the asymptotic range and it represents
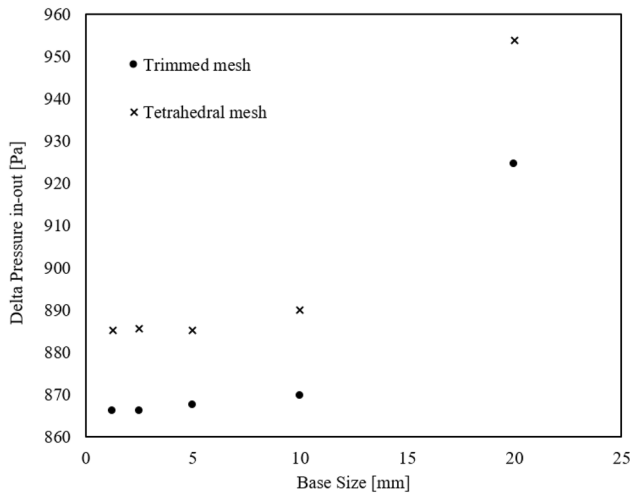
Fig. 3 Mesh sensitivity study for trimmed and tetrahedral meshes. Real geometry model

Table 2 Summarizing parameters for the mesh sensitivity study

	Base size (mm)	GCI	ΔP (Pa)	Number of cells
Tetrahedral mesh	2.5	3.03×10^{-5}	885.1	9,461,949
	5.0	4.80×10^{-4}	885.4	2,314,077
Trimmed mesh	2.5	1.44×10^{-3}	866.1	4,179,352
	5.0	2.88×10^{-3}	867.5	1,022,130

Real geometry model

the best compromise between computational cost and the accuracy of the results.

4 Results and discussion

In the following section, the influence of the mesh typology on both the computational cost and the obtained results is firstly investigated. The ΔP between the inlet and the outlet is used as reference parameter to compare results. Moreover, in order to assess the numerical model adopted, the axial velocities are compared with literature data [14]. Finally, the results obtained with the porous baffle interface are reported and analysed.

4.1 Tetrahedral *vs* trimmed mesh

In order to ensure the quality of the mesh generated with the base size chosen on the basis of the sensitivity study and the settings reported in the Material and Methods Section for the refinement area and the boundary layer, in Table 3 volume change, skewness angle, Chevron quality indicator and face validity data for both the trimmed and the tetrahedral mesh are summarized. The tetrahedral mesh has a high quality as it does not present Chevron cells, has lower skewness angles and a more homogenous volume change. However, the trimmed mesh present just the 0.006% of the cells with a volume change lower than 0.01 and does not have cells with skewness angle higher than 85°, that represent the limits for bad cells [19]. Moreover, just the 0.004% of the cells are identified as Chevron ones.

Considering the computational cost, Table 4 reports the cells number and the CPU (Central Processor Unit) time needed to lead the convergence criteria (residuals in the order of 10^{-5}, lead for both the model in 1000 iterations) for both the mesh typologies. The hardware used for the

Table 3 Trimmed *vs* tetrahedral mesh: mesh quality data

	Trimmed mesh		Tetrahedral mesh	
Max volume change	1.00		1.00	
Min volume change	0.001		0.13	
Volume change ranges: cell percentage	$0.001 \leq V < 0.01$	0.006%	$0.13 \leq V \leq 1.00$	100%
	$0.01 \leq V < 0.10$	1.41%		
	$0.10 \leq V \leq 1.00$	98.58%		
Max skewness angle	84.79°		74.58°	
Min skewness angle	0.33°		0.89°	
Skewness angle ranges: cell percentage	$0.33° \leq \Theta < 40°$	96.05%	$0.89° \leq \Theta < 35°$	82.19%
	$40° \leq \Theta < 80°$	3.95%	$35° \leq \Theta < 70°$	17.81%
	$\Theta \geq 80°$	0.003%	$\Theta \geq 70°$	0.00%
Chevron indicator: cell percentage	0.004	99.99%	0.004	100%
	0.99	0.004%		
Face validity: cell percentage	1.00	100%	1.00	100%

Table 4 Trimmed *vs* tetrahedral mesh: computational costs

	Number of cells (–)	CPU time (s)
Trimmed mesh	1,022,130	17,903
Tetrahedral mesh	2,314,077	81,492

Real geometry model

computations has the following characteristics: one physical processor Intel(R) Core(TM) i7-8565U CPU @ 1.80 GHz 1.99 GHz with four cores and 8 logical processors, an installed RAM (Random Access Memory) of 16.0 GHz and a GPU (Graphics Processing Unit) NVIDIA GeForce MX250 with 2.0 GB of dedicated memory. The trimmed mesh allows to use lower cells number and consequently to reduce the computational cost of about 78% in respect to the tetrahedral mesh.

A perusal of Fig. 4 shows that the wall y^+ values obtained with both the meshes are less than 1; this confirms the choice to perform the computations without the use of the wall functions.

To assess the adopted numerical model, in Fig. 5 a comparison is made between the axial velocities calculated and the one reported in [14]. It can be observed that both axial velocities calculated with tetrahedral and trimmed mesh are in line with the literature data [14]. The only appreciable difference is represented by the flow fluctuation captured along the outer pipe with the adopted model in respect to the literature one: this is due to a greater refinement area sets around the perforate pipe in the presented work.

Figure 6 reports the velocity field obtained with both the meshes on the symmetry plane: the only difference that can be noticed is represented by the flow through the holes that is captured in a different way with the two meshes. However, considering the ΔP between the inlet and the outlet, the results obtained with the two different meshes differs only by about 2%: 867 and 885 Pa are the ΔP for the trimmed and tetrahedral mesh respectively. Moreover, a perusal of Fig. 7 shows how both the meshes well capture the pressure drop caused by the perforated pipe and the flow fluctuation through the holes.

Even if a proper validation of the models has not been performed due to the lack of experimental measurements, a comparison, in terms of pressure loss caused by the perforated pipe, between literature data [14] and numerical results obtained in this work is addressed (Table 5) to further ensure the accuracy of the results. Literature data taken as reference has been validated against experimental measurements [14],
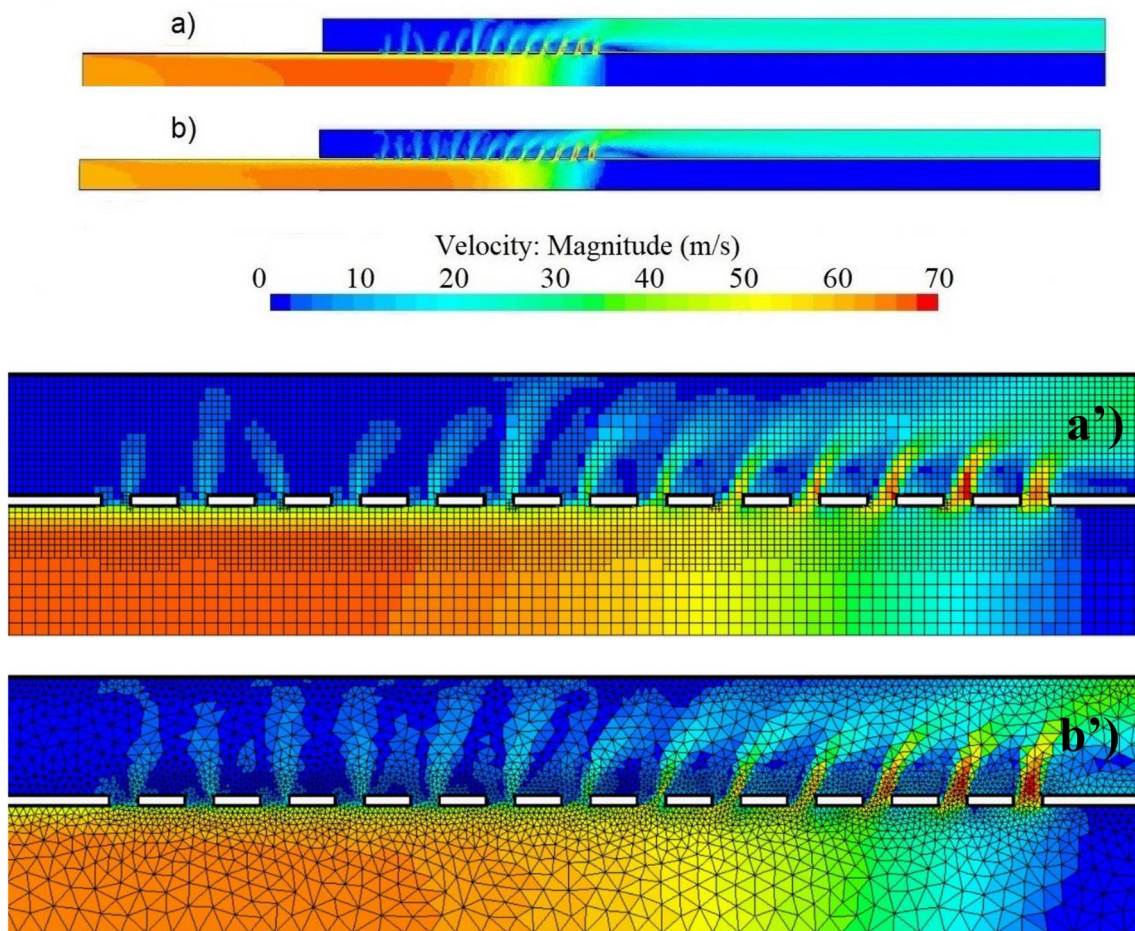

Fig. 4 Wall y^+ value along the domain: **a** trimmed mesh, **b** tetrahedral mesh. Real geometry model
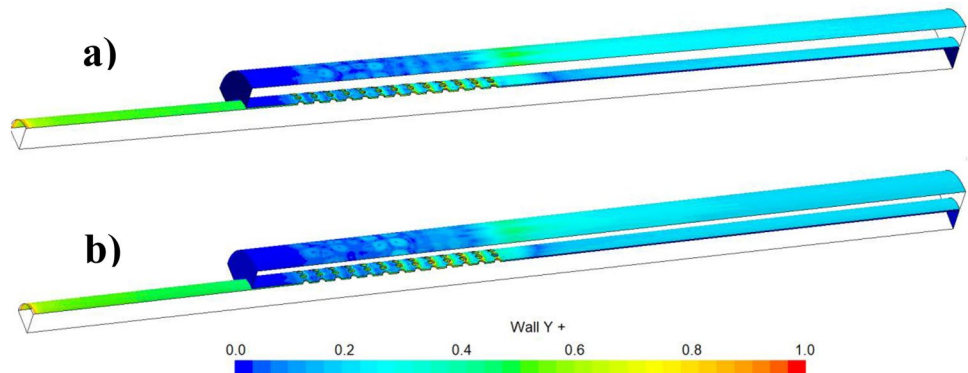
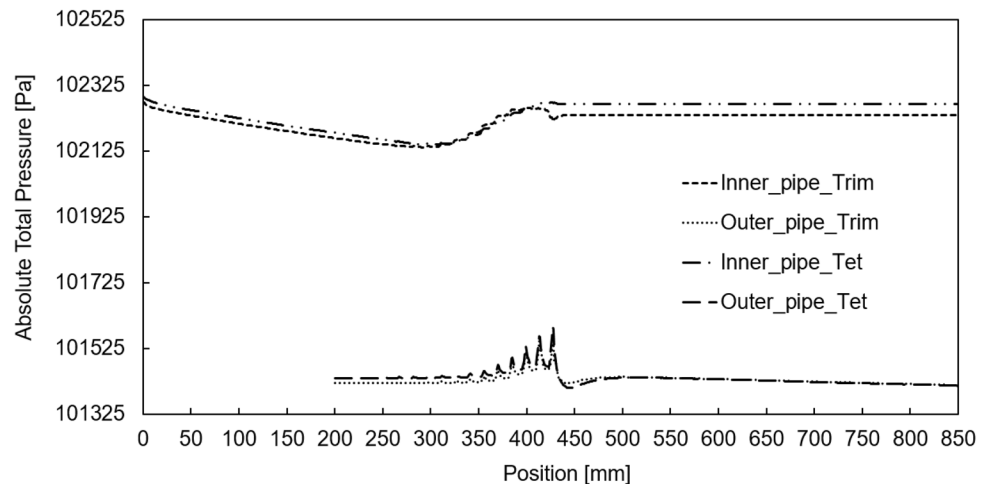**Fig. 5** Comparison between axial velocities. Real geometry model
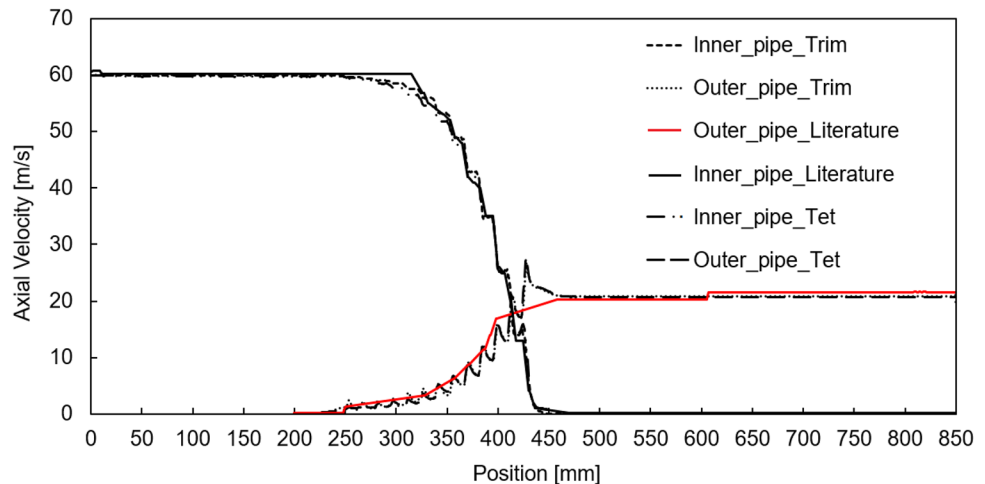
Fig. 6 Comparison of velocity field on symmetry plane: **a** tetrahedral mesh; **b** trimmed mesh; **a′**, **b′** zoom on the perforated pipe

Fig. 7 Trimmed *vs* tetrahedral mesh: comparison of absolute total pressures. Real geometry model

thus the good fitting with the numerical results obtained with both the models with trimmed and tetrahedral mesh (− 1.4% and +0.6% respectively) ensure the reliability and the accuracy of the presented results. The literature pressure loss caused by the perforated pipe (ΔP between inlet and

outlet cross section of perforated pipe) has been calculated considering the procedure explained in section "Cross flow expansion" of the paper taken as Ref. [14].

So, considering the small variation in terms of ΔP (both between inlet and outlet and caused by the perforated pipe)

Table 5 Trimmed *vs* tetrahedral mesh *vs* literature data: comparison between perforated pipe pressure loss

	Trimmed mesh	Tetrahedral mesh	Literature
ΔP (Pa)	858	875	870
Difference (%)	− 1.4	+ 0.6	

between the two mesh typology, the lesser computational burden and the small difference in terms of mesh quality, the trimmed mesh is chosen as the best one. For this reason, the trimmed mesh is used to investigate the porous baffle interface.
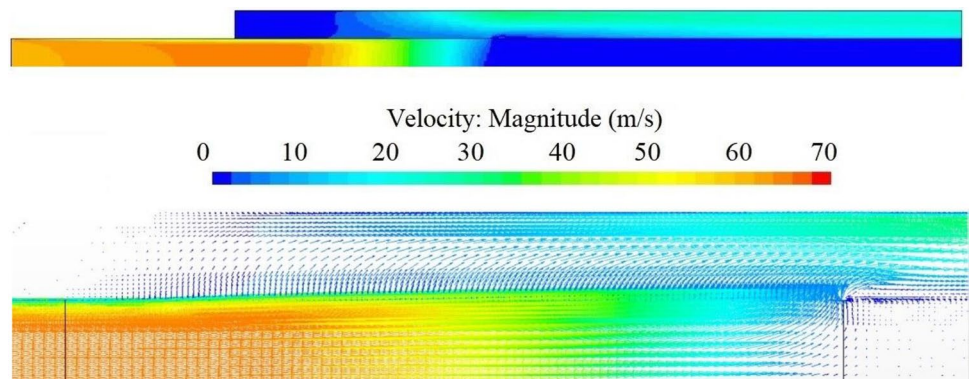
4.2 Porous baffle interface

In the model that use the porous baffle interface to model the perforated pipe, also the solid walls of the inner pipe (Fig. 1) are modelled using a baffle interface (not porous in this case). As previous mentioned, the geometry is discretized using the trimmed mesh (Fig. 8), with the same setting adopted for the real geometry model, they satisfy mesh sensitivity study and results accuracy as reported in a previous work [20]. The cells number and the CPU time needed to calculate 1000 iterations, necessary to lead the convergence criteria (i.e. residuals of the order of 10^{-5}),

are 907,628 and 17,545 s respectively. This simplified model allows to reduce the cells number of about 11% and the CPU time of about 2% in respect to the real geometry model with the trimmed mesh.

Looking at Fig. 9, that reports the velocity field developed with the porous baffle interface, noticeable is the difference compared to the field with the entire geometry (Fig. 6) along the porous pipe. As a matter of fact, the porous baffle is crossed by the flow along the entire length and the effects of the holes cannot be reproduced.

The comparison reported in Fig. 10 highlight the differences with the real geometry model in terms of axial velocity and absolute total pressure along the muffler. With the baffle interface model the ΔP between inlet and outlet is equal to 986 Pa, higher than that obtained with the real geometry model of about 14%.

The flow through the baffle is strictly related to the settings of the resistance parameters: in this work the Darcy–Forchheimer relation and the Ergun's equation are used to calculate their value (Eqs. 2–5), as reported in "Materials and methods" section. In order to reduce the difference between the pressure drop obtained with the real geometry model and the porous baffle interface one, the β coefficient has been varied. Nevertheless, no satisfactory results are reached; it has to be taken into account that the adopted theory is an approximation and that a numerical error could be introduced by the porous baffle interface.

Fig. 8 Baffles geometry's mesh, zoom on the porous baffle interface
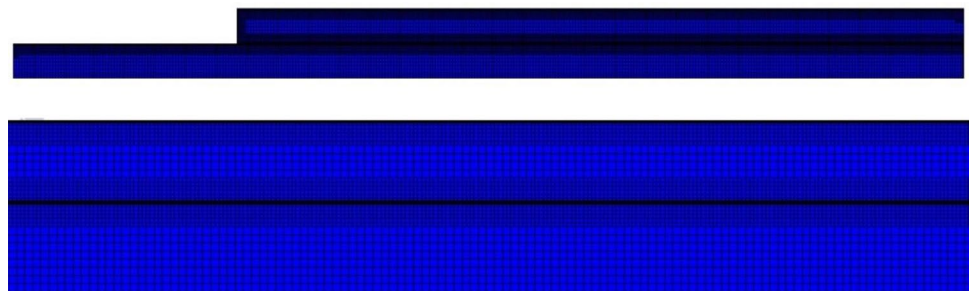
Fig. 9 Velocity field with porous baffle interface, zoom on the perforated pipe with streamlines reported

Velocity: Magnitude (m/s)

0   10   20   30   40   50   60   70

Fig. 10 Real geometry *vs* porous baffle interface models: comparison of axial velocities and absolute total pressures
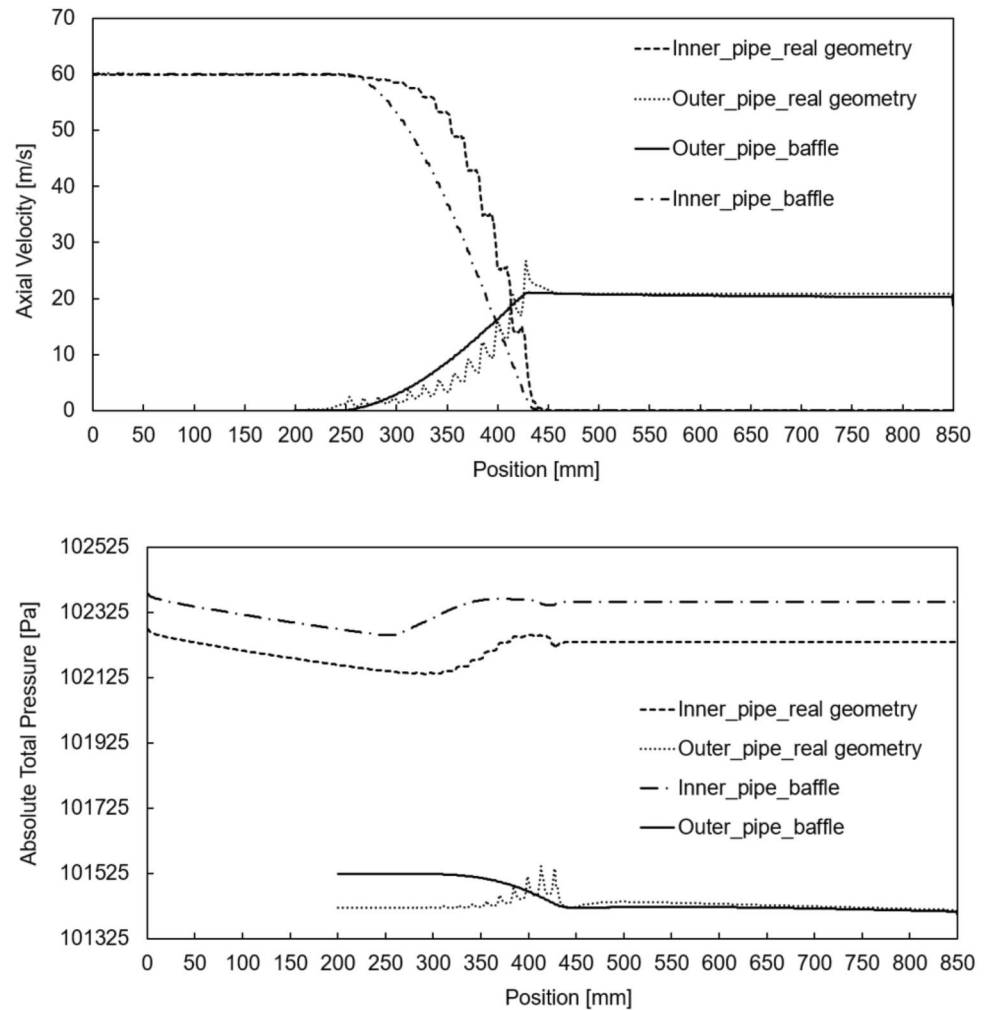
5 Conclusion

Numerical modelling is widely used to study mufflers performances. Nevertheless, it is not possible to find in literature general guidelines for the construction of the model. So, in this study a comparison between the use of trimmed and tetrahedral mesh in the flow analysis inside mufflers has been firstly performed. Then, with the mesh typology that represent a good compromise between numerical cost and accuracy of the results, the use of porous baffle interface to model the perforated pipes has been investigated with the aim to develop an easier numerical model.

The study highlights that the trimmed mesh allows to reach same results of the tetrahedral mesh (about 2% difference in terms of ΔP), but significantly reducing the computational cost: the trimmed mesh implies 55% less cells number and 78% lower CPU time.

The porous baffle interface simplifies the drawing and the meshing phases of the numerical model construction, as the holes has not to be drawn and meshed. Moreover,

the use of the porous interface allows to easy study different mufflers configurations (i.e. different holes geometries and number); to change the characteristics of the perforations and the influence they have on the flow that pass through them, it is sufficient to set different resistance parameters for the interface. Nevertheless, the obtained ΔP is higher of about 14% than the one obtained with the real geometry model (Fig. 10). The porous baffle interface introduces a numerical error and not reduce significantly the time needed to obtain a result (2% CPU time less than the real geometry model), but its usage could be useful in an early design phase for a comparative analysis between different muffler configurations.

In future works other strategy have to be tested to model perforated components: an example can be the use of a porous zone.

Declarations

Conflict of interest The authors have no conflicts of interest to declare that are relevant to the content of this article.

Data availability All data are reported in the text or referenced.

Code availability Software application.

References

1. IMO, resolution MSC.337(91), code on noise levels on board ships (2012)
2. EU, Commission Directive 1999/101/EC of 15 December 1999 adapting to technical progress Council Directive 70/157/EEC relating to the permissible sound level and the exhaust system of motor vehicles (1999)
3. R.D. Nazirkar, S.R. Meshram, A.D. Namdas, S.U. Navagire, S.S. Devarshi, Design & optimization of exhaust muffler & design validation. Int. J. Mech. Prod. Eng. 2 (2014)
4. Y. Chen, L. Lv, Design and evaluation of an Integrated SCR and exhaust Muffler from marine diesels. J. Mar. Sci. Technol. **20**, 505–519 (2015). https://doi.org/10.1007/s00773-014-0302-1
5. C.-N. Wang, C.-C. Tse, S.-C. Chen, Flow induced aerodynamic noise analysis of perforated tube mufflers. J. Mech. **29**, 225–231 (2013). https://doi.org/10.1017/jmech.2012.133
6. P.C. Rao, B.M. Varma, Muffler design, development and validation. Methods **5**, 14 (2007)
7. S. Barua, S. Chatterjee, CFD analysis on an elliptical chamber muffler of a CI engine. Int. J. Heat Technol. **37**, 613–619 (2019). https://doi.org/10.18280/ijht.370232
8. L. Liu, Z. Hao, C. Liu, CFD analysis of a transfer matrix of exhaust muffler with mean flow and prediction of exhaust noise. J. Zhejiang Univ. Sci. A. **13**, 709–716 (2012). https://doi.org/10.1631/jzus.A1200155
9. J.M. Middelberg, T.J. Barber, S.S. Leong, K.P. Byrne, E. Leonardi, Computational fluid dynamics analysis of the acoustic performance of various simple expansion chamber mufflers. In: Proceedings of ACOUSTICS 6 (2004)
10. J.M. Middelberg, T.J. Barber, S.S. Leong, K.P. Byrne, E. Leonardi, CFD Analysis of the Acoustic and Mean Flow Performance of Simple Expansion Chamber Mufflers, in: Noise Control Acoust., ASMEDC, Anaheim, pp. 151–156 (2004). https://doi.org/10.1115/IMECE2004-61371.
11. S.V. Narasimhan, S. Mahesh, M. Sivan, S.S. Nair, CFD case studies on the acoustic performance and backpressure changes on modified reactive mufflers. In: Chennai, p. 020005 (2020). https://doi.org/10.1063/5.0025346.
12. P.C. Mishra, S.K. Kar, H. Mishra, Effect of perforation on exhaust performance of a turbo pipe type muffler using methanol and gasoline blended fuel: a step to NOx control. J. Clean. Prod. **183**, 869–879 (2018). https://doi.org/10.1016/j.jclepro.2018.02.236
13. R.S. Nursal, A.H. Hashim, N.I. Nordin, M.A.A. Hamid, R. Danuri, CFD analysis on the effects of exhaust backpressure generated by four-stroke marine diesel generator after modification of silencer and exhaust flow design. J. Eng. Appl. Sci. **12**, 11 (2017)
14. S.N. Panigrahi, M.L. Munjal, Backpressure considerations in designing of cross flow perforated-element reactive silencers. Noise Control Eng. J. **55**, 504 (2007). https://doi.org/10.3397/1.2817808
15. A. Berg, Numerical and experimental study of the fluid flow in porous medium in charging process of stratified thermal storage tank, Master of Science Thesis, KTH School of Industrial Engineering and Management Energy Technology, 2013.
16. M.A. Kizilaslan, E. Demirel, M.M. Aral, Effect of porous baffles on the energy performance of contact tanks in water treatment. Water **10**, 1084 (2018). https://doi.org/10.3390/w10081084
17. M.D.M. Innocentini, V.R. Salvini, A. Macedo, V.C. Pandolfelli, Prediction of ceramic foams permeability using Ergun's equation. Mater. Res. **2**, 283–289 (1999). https://doi.org/10.1590/S1516-14391999000400008
18. L. Kwaśniewski, Application of grid convergence index in FE computation. Bull. Pol. Acad. Sci. Tech. Sci. (2013). https://doi.org/10.2478/bpasts-2013-0010
19. Star-CCM+ 2020.2 User Manual (n.d.).
20. G. Kyaw Oo D'Amore, F. Mauro, Numerical study on modelling perforated elements using porous baffle interface and porous region. J. Eng. Des. Technol. **10**, 20 (2021). https://doi.org/10.1108/JEDT-07-2021-0356